Physics and Imaging in Radiation Oncology 5 (2018) 102–107

Contents lists available at ScienceDirect

Physics and Imaging in Radiation Oncology

journal homepage: www.elsevier.com/locate/phro

Original Research Article

Analysis of intra-fraction prostate motion and derivation of duration-dependent margins for radiotherapy using real-time 4D ultrasound

Eric Pei Ping Pang[a,b,*], Kellie Knight[b], Qiao Fan[d], Sheena Xue Fei Tan[a], Khong Wei Ang[a], Zubin Master[a], Wing-Ho Mui[e], Ronnie Wing-Kin Leung[e], Marilyn Baird[b], Jeffrey Kit Loong Tuan[a,c]

[a] Division of Radiation Oncology, National Cancer Centre Singapore, 11 Hospital Drive, Singapore 169610, Singapore
[b] Faculty of Medicine, Nursing and Health Sciences, Department of Medical Imaging & Radiation Sciences, Monash University, Wellington Road, Clayton, VIC 3800, Australia
[c] Duke-NUS Graduate Medical School, 8 College Road, Singapore 169857, Singapore
[d] Centre for Quantitative Medicine, Duke-NUS Medical School, 8 College Road, Singapore 169857, Singapore
[e] Tuen Mun Hospital, 23 Tsing Chung Koon Road, Tuen Mun, New Territories, Hong Kong

ARTICLE INFO

Keywords:
Prostate
Intra-fraction movement
4D Clarity ultrasound system
Real-time tracking
Margins

ABSTRACT

Background and purpose: During radiotherapy, prostate motion changes over time. Quantifying and accounting for this motion is essential. This study aimed to assess intra-fraction prostate motion and derive duration-dependent planning margins for two treatment techniques.

Material and methods: A four-dimension (4D) transperineal ultrasound Clarity® system was used to track prostate motion. We analysed 1913 fractions from 60 patients undergoing volumetric-modulated arc therapy (VMAT) to the prostate. The mean VMAT treatment duration was 3.4 min. Extended monitoring was conducted weekly to simulate motion during intensity-modulated radiation therapy (IMRT) treatment (an additional seven minutes). A motion-time trend analysis was conducted and the mean intra-fraction motion between VMAT and IMRT treatments compared. Duration-dependent margins were calculated and anisotropic margins for VMAT and IMRT treatments were derived.

Results: There were statistically significant differences in the mean intra-fraction motion between VMAT and the simulated IMRT duration in the inferior (0.1 mm versus 0.3 mm) and posterior (−0.2 versus −0.4 mm) directions respectively ($p \ll 0.01$). An intra-fraction motion trend inferiorly and posteriorly was observed. The recommended minimum anisotropic margins are 1.7 mm/2.7 mm (superior/inferior); 0.8 mm (left/right), 1.7 mm/2.9 mm (anterior/posterior) for VMAT treatments and 2.9 mm/4.3 mm (superior/inferior), 1.5 mm (left/right), 2.8 mm/4.8 mm (anterior/posterior) for IMRT treatments. Smaller anisotropic margins were required for VMAT compared to IMRT (differences ranging from 1.2 to 1.6 mm superiorly/inferiorly, 0.7 mm laterally and 1.1–1.9 mm anteriorly/posteriorly).

Conclusions: VMAT treatment is preferred over IMRT as prostate motion increases with time. Larger margins should be employed in the inferior and posterior directions for both treatment durations. Duration-dependent margins should be applied in the presence of prolonged imaging and verification time.

1. Introduction

Intensity-modulated radiation therapy (IMRT) and volumetric-modulated arc therapy (VMAT) for the treatment of prostate cancer are widely practiced. Both techniques achieve a highly conformal dose distribution, enabling the sparing of surrounding normal tissues whilst delivering the high therapeutic doses. Several papers [1–3] have reported shorter VMAT treatment times compared to routine seven-or nine-field IMRT.

Image guidance allows setup position verification, improves treatment delivery accuracy and eliminates gross errors. With appropriate image guidance, the risk of adverse side effects to organ-at-risk (OARs) can be reduced [4]. Pre-treatment cone-beam computed tomography (CBCT) to correct for setup errors is common, however this only provides a snapshot of the prostate position during the scan and does not provide real-time intra-fraction monitoring of the prostate during the image verification and treatment phases. Intra-fraction motion has previously been rudimentarily calculated based on pre- and post- CBCT

* Corresponding author at: Division of Radiation Oncology, National Cancer Centre Singapore, 11 Hospital Drive, Singapore 169610, Singapore.
E-mail address: eric.pang.p.p@nccs.com.sg (E.P.P. Pang).

https://doi.org/10.1016/j.phro.2018.03.008
Received 20 November 2017; Received in revised form 15 March 2018; Accepted 15 March 2018
2405-6316/ © 2018 The Authors. Published by Elsevier B.V. on behalf of European Society of Radiotherapy & Oncology. This is an open access article under the CC BY-NC-ND license (http://creativecommons.org/licenses/BY-NC-ND/4.0/).

image registrations [5–8]. More recently there has been a paradigm shift towards the yield of real-time motion data using non-ionizing radiation modalities such as electromagnetic transponders (EMT) and four-dimension (4D) transperineal ultrasound (TPUS).

Numerous studies [9–17] have reported the magnitude and trend of intra-fraction prostate motion using EMT. EMT monitoring is limited to acquiring geometrical coordinates of the transponders and lacks information on soft tissue boundaries of the prostate and surrounding OARs. There are also a limited number of small studies [18,19] (n = 6–10) utilising auto-scanning TPUS for monitoring of intra-fraction motion. The fundamental tracking algorithm of the TPUS system is intensity-based using normalised cross-relation as the cost-function that accounts for surrounding pixels within a 2 mm boundary from the prostate contour [20]. Tracking accuracy of TPUS and EMT has been shown to be comparable within sub-millimetre [13,20–22]. Abramowitz et al. [23] reported agreement of < 0.6 mm maximum distance variation in motion tracking between TPUS and EMT. These previous TPUS studies employed small sample sizes and did not compare margins derived between VMAT and IMRT using patients as their own control.

This study aimed to assess and compare intra-fraction prostate motion between VMAT and IMRT by conducting a motion-time analysis. The study hypothesized that there was a difference in the mean paired prostate motion between VMAT and IMRT in each direction. Duration-dependent planning margins were subsequently derived for both techniques. To our knowledge, this is the first paper to assess differences in observed intra-fraction motion of the prostate using paired TPUS motion data, and the first on an Asian cohort.

2. Material and methods

Ethics approval was obtained in November 2014 and the study registered on the National Institute of Health (NIH) clinical trial registry (ID: NCT02408497). We prospectively recruited 60 consecutive patients from the radiotherapy departments at the National Cancer Centre Singapore (NCCS) and Tuen Mun Hospital, Hong Kong (TMH). All patients (55 from NCCS and 5 from TMH) provided informed consent and received standard VMAT treatment. Patient characteristics are summarised in Table S1 (in supplementary material).

2.1. Patient setup and positioning

Patients were positioned using a knee rest with legs slightly spread (Fig. S1 in supplementary material). Patients followed an individual bladder preparation of 2–3 cups of water (400–600 ml) 30 min before treatment. No specific dietary advice or rectal emptying instructions were given, but patients were encouraged to empty their bowels prior to each fraction. The total imaging and beam-on time required to deliver the prescribed treatment was recorded and the Clarity® system positioning graph was documented for offline analysis against the planning margin employed (Fig. S2 in supplementary material).

2.2. Workflow of 4D TPUS Clarity® system

Before using the 4D Clarity® TPUS system, an infrared-red optical camera was calibrated against the calibration phantom to ensure accuracy of the tracking process during treatment. Due to limited resources, only one 4D Clarity® ultrasound system was located inside our IGRT dedicated treatment room. An autoscan probe (2D frame mode) was held in place for a continuous sweep to acquire a 3D reconstructed dataset [20]. The patient setup workflow process has previously been described [24]. On the first fraction, a routine pre-treatment CBCT was acquired and the patient's position corrected. A reference TPUS scan was then acquired to capture the imaging and treatment position of the prostate. These TPUS images were transferred to a standalone Automatic Fusion and Contouring (AFC) workstation and registered with the planning CT images [24]. The prostate was contoured offline and used to define the reference positioning volume (RPV) (i.e. prostate gland).

For subsequent fractions, once patients were set up in the treatment position, the ultrasound probe was positioned with reference to the initial probe position to acquire a pre-treatment ultrasound scan. The time taken for the daily imaging regime prior to commencement of treatment was recorded, together with the observed real-time intra-fraction prostate motion.

To simulate prostate motion during an IMRT technique, once weekly all patients remained in the treatment position for an additional seven minutes. This additional seven minutes was based on a retrospective review conducted in our department to determine the average treatment time for VMAT vs IMRT prostate treatments from January to December 2013 (n = 105). This extended tracking time enabled a comparison of intra-fraction prostate motion between VMAT and the simulated IMRT duration for each patient.

2.3. Image verification and treatment time

Daily pre-treatment CBCT was used to verify and correct patient position prior to treatment delivery in this study. Image registration was performed using the integrated algorithm on the Varian on-board imager (OBI) console. Automatic registration using the bony anatomy was performed first, followed by manual fine-tuning to match the primary prostate ± SV volumes. If the difference between the bony and soft tissues registration was within 5 mm, the resultant shift was applied, otherwise the patient was repositioned and re-verified. A total of 1744 treatment fractions from 55 patients demonstrated the mean imaging (4.2 min) and VMAT times (3.4 min) required for prostate radiotherapy (Table S2 in supplementary material).

2.4. Real-time intra-fraction monitoring

Intra-fraction monitoring was continuous and divided into two sequential phases: the imaging and verification phase, followed by the treatment delivery phase. Motion was observed in real-time at a frame rate of 3–4 data points per second depending on the depth and scan angle for each patient. The imaging and verification phase was defined from the time the radiation therapists left the treatment room until the time couch corrections (after CBCT acquisition and assessment) were applied. The treatment phase was defined from the time the couch position application was applied until the beam-off time. For the comparison between VMAT and IMRT treatments, motion data was normalised at the beginning of the treatment phase (i.e. the image frame at that time point was used as the reference position). However, when calculating intra-fraction margins specific to motion detected during the entire imaging and treatment process, motion data was normalised from the start of the imaging and verification phase, thus allowing the true motion related to imaging and treatment duration to be calculated.

2.5. Motion-time trend analysis

Intra-fraction motion was analysed for 55 patients (the imaging phase of TMH patients (n = 5) was not recorded). The entire duration, including the imaging phase, was analysed to elicit the tendency of motion with a temporal resolution of 30 s for an eight-minute period (i.e. the length of a VMAT treatment). A motion-time trend analysis from 1744 monitoring sessions generated a boxplot series (each representing a 30-s period) that illustrated the trend of observed motion for the cohort (n = 55) (Figs. S3–S5 in supplementary material).

2.6. Statistical analysis

A paired *t*-test was used to compare the magnitude of intra-fraction motion between matched IMRT and VMAT sessions (n = 60). The

analysis was performed using PASW for Windows, version 20.0 (SPSS Inc, Chicago, IL). Next, a correlation test was carried out to investigate the impact of overall duration on the magnitude of the observed intra-fraction motion. This was performed using mixed models for motion trajectory fitted for 55 individuals, incorporating both an intercept and a slope (polynomial time terms with respect to patient) in the fixed and random effects. The analysis was performed using the *nlme* package in R software v.3.2.5. A margin calculation using the van Herk's margin recipe ($2.5\Sigma + 1.64((\sigma^2 + \sigma_p^2)^{1/2} - \sigma_p)$) was performed to estimate the required margin for IMRT and VMAT treatments [25]. Fig. S6 (supplementary material) illustrates the data used for margin calculation. An anisotropic margin in each direction was calculated to account for mean intra-fraction motion.

3. Results

3.1. Comparison of intra-fraction motion between VMAT and IMRT

The observed intra-fraction motion was normally distributed (Fig. S7 in supplementary material). As hypothesised, there was a statistically significant difference in the observed mean intra-fraction motion between VMAT and simulated IMRT treatment durations (i.e. 389 pairs of matched data from 60 patients) in the inferior (0.1 mm versus 0.3 mm) and posterior (−0.2 versus −0.4 mm) directions respectively ($p \ll 0.01$) (Table 1). A separate weighted *t*-test revealed statistically significant differences between the mean motion accounting for the variation of motions (i.e. standard deviations) (Table S3 in supplementary material).

3.2. Motion-time trend analysis

The overall time effects on motion trajectory were significant in the Superior/Inferior and Anterior/Posterior direction ($p \ll 0.01$), but not significant in Left/Right direction ($p = 0.33$). The trend of mean intra-fraction motion for each individual over time is presented in Fig. 1.

3.3. Recommended duration-dependent margin

The generated minimum recommended margins (symmetrical within superior/inferior, lateral and anterior/posterior axes) were 2.2 mm, 0.8 mm and 2.3 mm for VMAT and 3.6 mm, 1.5 mm, 3.8 mm for IMRT (Table 2). Table 3 illustrates the derived anisotropic margin expansions. The anisotropic margins required for VMAT were much smaller than for IMRT (differences ranging from 1.2 to 1.6 mm superiorly/inferiorly, 0.7 mm laterally and 1.1–1.9 mm anteriorly/posteriorly).

Table 1
Illustrates the paired *t*-test results of the observed intra-fraction motion between the matched VMAT and IMRT treatments (n = 60).

		Paired differences (mm)					Sig. (2-tailed)
		Mean	Std. Deviation*	Std. Error Mean	95% Confidence Interval of the Difference		
					Lower	Upper	
Pair 1	Mean_x (Inf/Sup)	−.2	.7	.03	−.22	−.09	≪0.01
Pair 2	Mean_y (Lt/Rt)	0	.5	.03	−.07	.04	.53
Pair 3	Mean_z (Ant/Post)	.2	.8	.04	.13	.29	≪0.01

* SD values were based on paired VMAT and IMRT data from the same session (n = 389).

4. Discussion

The duration required for imaging and verification (4.2 min) exceeding the duration of a typical VMAT treatment (3.4 min) can be attributed to the time needed to acquire and process CBCT images. This study has illustrated the relationship of intra-fraction prostate motion with time. The 4D TPUS system has the potential to reduce overall imaging and treatment times, as well as to reduce patient's exposure to ionizing radiation if used as the primary verification tool.

When calculating margins, it was pertinent to account for intra-fraction motion that occurred during the imaging phase as well as during treatment delivery. Fig. 1 illustrated the motion within each plane, with the majority of the observed motions < 5 mm. Baker et al. [18] investigated prostate motion once a week (n = 10) for a duration of 2–2.5 min after treatment delivery using TPUS and reported a maximum 2.8 mm motion posteriorly. However, tracking commenced post-treatment and did not include compounded motion that occurred during the imaging and treatment phases. The impact of imaging time on prostate motion during the actual treatment phase was observed with correlation tests revealing a trend towards larger intra-fraction motion in the Superior/Inferior and Anterior/Posterior directions over time (Figs. S3 and S5). The prolonged duration of IMRT also explains the significant difference between VMAT and IMRT as reported in Table 1.

The ability of the 4D TPUS system to provide continuous real-time tracking of the prostate allowed the derivation of duration-dependent margins. In Table 1, the corresponding mean paired difference between IMRT and VMAT was 0.2 mm (i.e. anterior/posterior), however the difference was 0.4 mm (i.e. −0.6 mm and −1.0 mm) in Table 2. This was because the values in Table 1 were calculated on paired VMAT and IMRT data from the same session, whereas, Table 2 incorporated all the other VMAT sessions when calculating the margins. From Table 2, it was apparent that the minimum margin required for all axes during IMRT treatment was significantly larger when compared to VMAT treatments. This can be directly attributed to the prolonged treatment duration for IMRT (with the assumption of minimal patient movement). After accounting for the population mean shifts, an anisotropic margin was derived for each technique in each direction. Since the observed mean intra-fraction prostate motion for both VMAT and IMRT techniques trended towards the inferior and posterior directions, a larger margin was required for these directions (Table 3). The mean intra-fraction motion in the left/right direction was relatively stable and hence a symmetrical margin expansion was recommended. The results of the direction of the observed mean intra-fraction motion from this study were in accordance to the previous findings by Cramer et al. [26] who tracked the prostate gland using implant EMT. Based on our VMAT data, σ was approximately 1 mm, which would result in a value of 0.2σ rather than 0.7σ if a simplified linear van Herk's margin formula was used [27]. As such, the use of 0.7σ could result in a slightly overestimated margin. Therefore, the authors employed the original non-linear van Herk's margin formula $1.64((\sigma^2 + \sigma_p^2)^{1/2} - \sigma_p)$ for the random component which accounts for penumbra width (σ_p) of around 3.2 mm [25].

Inter-fraction setup error was not included in the margin derivation as it was corrected online using daily CBCT. It is pertinent to remember that the recommended margin expansion was based on the intra-fraction motion observed during both imaging and treatment phases. Therefore, the recommended minimum margin expansions from this study are only applicable to total treatment durations up to eight minutes (VMAT) and 15 min (IMRT).

The current prescribed margin around the prostate at NCCS (i.e. 1 cm all round and 6 mm posteriorly) could be reduced to allow sparing of more normal tissues and facilitate dose escalation treatment regimes. From our study, a minimum 5 mm anisotropic posterior margin was adequate to mitigate intra-fraction motion of the prostate for a period of 15 min. This is also sufficient to account for seminal vesicle mobility as

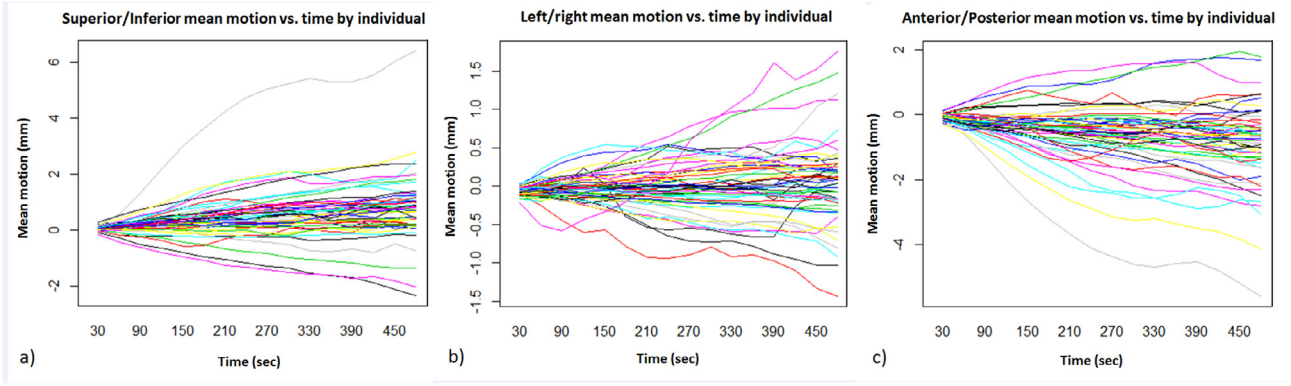

Fig. 1. Illustration of the mean intra-fraction motion for each individual with respect to the 30-s blocks in the a) Superior/Inferior, b) left/right and c) anterior/posterior directions.

Table 2
Illustrates the systematic and random values used to calculate the minimum recommended margins (symmetrical within each x, y and z directions).

	VMAT margin (mm)				IMRT margin (mm)			
	Population mean	Σ	σ	Margin formula*	Population mean	Σ	σ	Margin formula*
x (Inf/Sup)	0.5	0.74	1.13	2.2	0.7	1.21	1.48	3.6
y (Lt/Rt)	0.0	0.27	0.77	0.8	0.0	0.48	1.08	1.5
z (Ant/Post)	−0.6	0.77	1.27	2.3	−1.0	1.26	1.68	3.8

* Margin formula: $2.5\Sigma + 1.64((\sigma^2 + \sigma_p^2)^{1/2} - \sigma_p)$.

Table 3
Illustrates the derivation of the minimum recommended anisotropic margins for each direction after adjusting for the mean motions.

	VMAT margin (mm)			IMRT margin (mm)		
	Population mean	Symmetric within plane#	Anisotropic^	Population mean	Symmetric within plane#	Anisotropic^
Sup (−)	0.5	2.2	1.7	0.7	3.6	2.9
Inf (+)			2.7			4.3
Left (+)	0.0	0.8	0.8	0.0	1.5	1.5
Right (−)			0.8			1.5
Ant (+)	−0.6	2.3	1.7	−1.0	3.8	2.8
Post (−)			2.9			4.8

\# Expansion of margins symmetrically within each plane with reference to Table 2.
^ Expanding the margins unsymmetrically to derive the anisotropic margins within each plane.

reported by Sheng et al. [28]. Depending on the total time required for the prescribed imaging and treatment time, one may apply either the recommended VMAT (eight minutes) or IMRT (15 min) duration-dependent margin expansions. The margin expansion for SBRT of the prostate in NCCS prior to this study was 5 mm all round and 3 mm posteriorly. Despite the application of daily CBCT imaging and verification in the SBRT setting, we believe the role of tracking and a 15-min time-specific margin should be employed to ensure the desired treatment position is achieved Due to the increased dose per fraction and smaller margins employed in SBRT, in-treatment tracking would be appropriate and useful to address gross motion uncertainties especially at the posterior boundaries where a smaller than recommended minimum margin was used.

The authors have previously acknowledged the risk of systematic errors as the reference TPUS was acquired and registered offline with the planning CT images on the first day of treatment instead of at CT simulation [24]. The authors also acknowledge that tracking information in the present work cannot separate prostate motion from overall patient movement and all reported motion would be a combination of physical and internal motion.

Some pertinent factors need to be considered before the application of this margin in clinical practice. These include potential systematic errors (such as the delineation of the prostate by the radiation oncologist which has been conservatively estimated to be 2 mm [29]), inter- and intra-observer variations in CBCT and TPUS (if standalone) image registration, and uncertainties in positioning due to rotations of the prostate when only translational couch corrections are applied [30]. Most of these factors were not analysed in this study. Nonetheless, this paper has provided the systematic and random components of intra-fraction prostate motion that can be appropriately combined with other known sources of error to generate the final margins. Seminal vesicle motion, nor the use of endorectal balloons, was investigated in this study and their impact on PTV margins should be acknowledged. A recent paper by Sheng et al. [28] concluded a minimal isotropic margin expansion of 5 mm was adequate to account for intra-fraction motion of the seminal vesicles.

The margins we calculated could theoretically be reduced further if the time required for verification was reduced. The use of TPUS as a standalone verification imaging technique still requires further research together with a robust quality assurance testing program to perform image registration compared to CBCT. If clinically implemented, the penile bulb should be delineated given a potential increase in dose due to the probe pressure [31]. In addition, the value of the TPUS for tracking should be explored in the setting of proton treatment delivery to mitigate issues of range uncertainties. With the advancement in technology, SBRT delivery times are now relatively shorter due to

emergence of flattening-filter-free (FFF) or high dose rate capabilities. However, the application of duration-dependent margins is still applicable when a complex setup is used, prolonged image verification time persists, or in the proton setting, where beam waiting and re-verification can impact on the overall treatment time. Finally, not all radiotherapy centres will have access to state-of-the-art equipment (i.e. MRI-Linacs, flattening-filter-free beams) capable of advanced imaging and fast treatment delivery. Thus, TPUS and duration-dependent margins offer a cost-effective solution that might be suitable for all radiotherapy centres worldwide. In the absence of these to mitigate positioning uncertainties, the use of conservative margins or mid-treatment corrections remains the alternative for motion management strategies [32,33].

Ballhausen et al. [19] have suggested a linear relationship between duration of treatment and variance in prostate motion, consequently a fixed margin cannot be applied to optimally account for intra-fraction motion. This linear association can also be appreciated from Figs. S3–S5. Given the two calculated margin expansions at eight minutes and 15 min duration, the need for a 4D margin recipe is proposed to calculate the required margins in the event of extended duration beyond 15 min.

In conclusion, duration-dependent planning margins should be applied when using different treatment techniques. VMAT treatment is preferred as shorter treatment durations reduce prostate motion, thus requiring smaller planning margins. Larger anisotropic margins should be employed, particularly in the inferior and posterior directions of the prostate, due to the larger magnitude of observed motion in these directions. Prolonged imaging and verification times should be avoided to reduce prostate motion during actual treatment delivery. In the absence of intra-fraction motion correction, this study's contribution in advancing knowledge of prostate motion over time will increase confidence in the accurate delivery of treatment and allow for the application of duration-dependent planning margins to facilitate dose-escalated prostate radiation therapy.

Conflict of interest statement

The authors do not have any potential conflicts of interest.

Acknowledgements

The authors express their appreciation to Elekta Pte Ltd for providing the 4D TPUS Clarity equipment and in-house training. We thank Mr David Cooper, Clinical Researcher from Elekta Pte Ltd for the technical advice and validation of the output data from the Clarity US system. We would like to thank our Physics team (Dr James Lee and Ms Wendy Chow) for the technical support on installation and commission of the equipment. We also thank the radiation therapists involved in the treatment process. We are thankful for the IT support provided by Mr Gan Soon Ann and Mr Peter Huang, from the Department of Cancer Informatics, National Cancer Centre Singapore. The authors extend appreciation of clinical trial facilitation by Ms Ma Than Than and Ms Yeo Sook Kwan. We thank Ms Ong Whee Sze from the Division of Clinical Trial Epidemiology, National Cancer Centre Singapore, for her statistical support. We also thank Dr Aidan Sudbury from the School of Mathematical Sciences, Monash University, Australia, for his statistical advice. We thank Tuen Mun Hospital, Hong Kong, for their collaborative work; Mr Matthew Wong and Ms Tong Man for the administration support required for data collection and transfer.

Appendix A. Supplementary data

Supplementary data associated with this article can be found, in the online version, at http://dx.doi.org/10.1016/j.phro.2018.03.008.

References

[1] Palma D, Vollans E, James K, Nakano S, Moiseenko V, Shaffer R, et al. Volumetric modulated arc therapy for delivery of prostate radiotherapy: comparison with intensity-modulated radiotherapy and three-dimensional conformal radiotherapy. Int J Radiat Oncol Biol Phys 2008;72:996–1001.
[2] Tsai CL, Wu JK, Chao HL, Tsai YC, Cheng JCH. Treatment and dosimetric advantages between VMAT, IMRT, and Helical TomoTherapy in prostate cancer. Med Dosim 2011;36:264–71.
[3] Kopp RW, Duff M, Catalfamo F, Shah D, Rajecki M, Ahmad K. VMAT vs. 7-Field-IMRT: assessing the dosimetric parameters of prostate cancer treatment with a 292-patient sample. Med Dosim 2011;36:365–72.
[4] Vargas C, Yan D, Kestin LL, Krauss D, Lockman DM, Brabbins DS, et al. Phase II dose escalation study of image-guided adaptive radiotherapy for prostate cancer: use of dose-volume constraints to achieve rectal isotoxicity. Int J Radiat Oncol Biol Phys 2005;63(1):141–9.
[5] Steiner E, Georg D, Goldner G, Stock M. Prostate and patient intrafraction motion: impact on treatment time-dependent planning margins for patients with endorectal balloon. Int J Radiat Oncol Biol Phys 2013;86(4):755–61.
[6] Logadottir A, Korreman S, Petersen PM. Comparison of the accuracy and precision of prostate localization with 2D–2D and 3D images. Radiother Oncol 2011;98:175–80.
[7] Thomas SJ, Ashburner M, Tudor GS, Treeby J, Dean J, Routsis D, et al. Intra-fraction motion of the prostate during treatment with helical tomotherapy. Radiother Oncol 2013;109:482–6.
[8] Melancon AD, O'Daniel JC, Zhang L, Kudchadker RJ, Kuban DA, Lee AK, et al. Is a 3-mm intrafractional margin sufficient for daily image-guided intensity-modulated radiation therapy of prostate cancer? Radiother Oncol 2007;85:251–9.
[9] O'Shea TP, Garcia LJ, Rosser KE, Harris EJ, Evans PM, Bamber JC. 4D ultrasound speckle tracking of intra-fraction prostate motion: a phantom-based comparison with x-ray fiducial tracking using CyberKnife. Phys Med Biol 2014;59(7):1701–20.
[10] Tang S, Deville C, McDonough J, Tochner Z, Wang KK, Vapiwala N, et al. Effect of intrafraction prostate motion on proton pencil beam scanning delivery: a quantitative assessment. Int J Radiat Oncol Biol Phys 2013;87:375–82.
[11] Mayyas E, Chetty IJ, Chetvertkov M, Wen N, Neicu T, Nurushev T, et al. Evaluation of multiple image-based modalities for image-guided radiation therapy (IGRT) of prostate carcinoma: a prospective study. Med Phys 2013;40(4):041707.
[12] Wang KK, Vapiwala N, Bui V, Deville C, Plastaras JP, Bar-Ad V, et al. The impact of stool and gas volume on intrafraction prostate motion in patients undergoing radiotherapy with daily endorectal balloon. Radiother Oncol 2014;112(1):89–94.
[13] Kupelian P, Willoughby T, Mahadevan A, Djemil T, Weinstein G, Jani S, et al. Multi-institutional clinical experience with the Calypso System in localization and continuous, real-time monitoring of the prostate gland during external radiotherapy. Int J Radiat Oncol Biol Phys 2007;67(4):1088–98.
[14] Lin Y, Liu T, Yang W, Yang X, Khan MK. The non-Gaussian nature of prostate motion based on real-time intrafraction tracking. Int J Radiat Oncol Biol Phys 2013;87:363–9.
[15] Shelton J, Rossi PJ, Chen H, Liu Y, Master VA, Jani AB. Observations on prostate intrafraction motion and the effect of reduced treatment time using volumetric modulated arc therapy. Pract Radiat Oncol 2011;1(4):243–50.
[16] Shah AP, Kupelian PA, Willoughby TR, Langen KM, Meeks SL. An evaluation of intrafraction motion of the prostate in the prone and supine positions using electromagnetic tracking. Radiother Oncol 2011;99:37–43.
[17] Litzenberg DW, Balter JM, Hadley SW, Sandler HM, Willoughby TR, Kupelian PA, et al. Influence of intrafraction motion on margins for prostate radiotherapy. Int J Radiat Oncol Biol Phys 2006;65:548–53.
[18] Baker M, Behrens CF. Determining intrafractional prostate motion using four dimensional ultrasound system. BMC Cancer 2016;16:484.
[19] Ballhausen H, Li M, Hegemann NS, Ganswindt U, Belka C. Intra-fraction motion of the prostate is a random walk. Phys Med Biol 2015;60(2):549–63.
[20] Lachaine M, Falco T. Intrafractional prostate motion management with the Clarity autoscan system. Med Phys Int J 2013;1(1):72–80.
[21] O'Shea T, Bamber J, Fontanarosa D, van der Meer S, Verhaegen F, Harris E. Review of ultrasound image guidance in external beam radiotherapy part II: intra-fraction motion management and novel applications. Phys Med Biol 2016;61(8):R90–137.
[22] Trivedi A, Ashikaga T, Hard D, Archambault J, Lachaine M, Cooper DT, et al. Development of 3-dimensional transperineal ultrasound for image guided radiation therapy of the prostate: early evaluations of feasibility and use for inter- and intrafractional prostate localization. Pract Radiat Oncol 2017;7:e27–33.
[23] Abramowitz MC, Bossart E, Flook R, Wu X, Brooks R, Lachaine M, et al. Noninvasive real-time prostate tracking using a transperineal ultrasound approach. Int J Radiat Oncol Biol Phys 2012;84(3 Suppl):S133.
[24] Pang EPP, Knight K, Baird M, Tuan JKL. Inter- and intra-observer variation of patient setup shifts derived using the 4D TPUS Clarity system for prostate radiotherapy. Biomed Phys Eng Express 2017;3(2):025014.
[25] Sonke JJ, Lebesque J, van Herk M. Variability of four-dimensional computed tomography patient models. Int J Radiat Oncol Biol Phys 2008;70:590–8.
[26] Cramer A, Haile A, Ognjenovic S, Doshi T, Reilly W, Rubinstein K, et al. Real-time prostate motion assessment: image-guidance and the temporal dependence of intrafraction motion. BMC Med Phys 2013;13(1):4.
[27] van Herk M. Errors and margins in radiotherapy. Semin Radiat Oncol 2004;14(1):52–64.
[28] Sheng Y, Li T, Lee WR, Yin F-F, Wu QJ. Exploring the margin recipe for online adaptive radiation therapy for intermediate-risk prostate cancer: an intra-fractional seminal vesicles motion analysis. Int J Radiat Oncol Biol Phys 2017;98(2):473–80.

[29] Steenbakkers RJ, Duppen JC, Fitton I, Deurloo KE, Zijp L, Uitterhoeve AL, et al. Observer variation in target volume delineation of lung cancer related to radiation oncologist-computer interaction: a 'Big Brother' evaluation. Radiother Oncol 2005;77:182–90.
[30] Huang CY, Tehrani JN, Ng JA, Booth J, Keall P. Six degrees-of-freedom prostate and lung tumor motion measurements using kilovoltage intrafraction monitoring. Int J Radiat Oncol Biol Phys 2015;91:368–75.
[31] Mantel F, Richter A, Groh C, Lawrenz I, Weick S, Polat B, et al. Changes in penile bulb dose when using the Clarity transperineal ultrasound probe: a planning study. Pract Radiat Oncol 2016;6(6):e337–44.
[32] Kotte AN, Hofman P, Lagendijk JJ, van Vulpen M, van der Heide UA. Intrafraction motion of the prostate during external-beam radiation therapy: analysis of 427 patients with implanted fiducial markers. Int J Radiat Oncol Biol Phys 2007;69:419–25.
[33] Mutanga TF, de Boer HC, Rajan V, Dirkx ML, Incrocci L, Heijmen BJ. Day-to-day reproducibility of prostate intrafraction motion assessed by multiple kV and MV imaging of implanted markers during treatment. Int J Radiat Oncol Biol Phys 2012;83:400–7.